RSC Advances

This is an *Accepted Manuscript*, which has been through the Royal Society of Chemistry peer review process and has been accepted for publication.

Accepted Manuscripts are published online shortly after acceptance, before technical editing, formatting and proof reading. Using this free service, authors can make their results available to the community, in citable form, before we publish the edited article. This *Accepted Manuscript* will be replaced by the edited, formatted and paginated article as soon as this is available.

You can find more information about *Accepted Manuscripts* in the Information for Authors.

Please note that technical editing may introduce minor changes to the text and/or graphics, which may alter content. The journal's standard Terms & Conditions and the Ethical guidelines still apply. In no event shall the Royal Society of Chemistry be held responsible for any errors or omissions in this *Accepted Manuscript* or any consequences arising from the use of any information it contains.

ROYAL SOCIETY OF CHEMISTRY

www.rsc.org/advances

Cite this: DOI: 10.1039/c0xx00000x

www.rsc.org/xxxxxx

ARTICLE TYPE

Luminescence properties of $Ca_2Si_5N_8:Eu^{2+}$ prepared by gas-pressed sintering using BaF_2 as flux and cation substitution

Chuang Wang, Zhengyan Zhao, Xicheng Wang, Yanyan Li, Quansheng Wu, Yuhua Wang*

Received (in XXX, XXX) Xth XXXXXXXXX 20XX, Accepted Xth XXXXXXXXX 20XX
DOI: 10.1039/b000000x

Abstract

Eu^{2+} doped $Ca_2Si_5N_8$ phosphors were successfully prepared by gas-pressed sintering. The red-shift of the emission band from 608 nm to longer wavelength 622 nm of the $Ca_2Si_5N_8:Eu^{2+}$ phosphor under blue excitation has been achieved, and a large enhancement in the emission intensity has been obtained by using BaF_2. XRD data revealed that the lattice of $Ca_2Si_5N_8:Eu^{2+}$ was expanded with Ba^{2+} ions doping. XPS results suggested that there were more Eu^{2+} ions incorporated into the lattice of Ba^{2+} doped samples than those of the undoped samples. The doping effect of Ba^{2+} ions has been discussed in detail.

1. Introduction

Light emitting diode (LED)-based solid-state lighting has recently received worldwide attention, owing to the characteristics of high efficiency, simple structure, and long life. [1] The need for new phosphors arise in the past decade with the invention of the near-UV to blue emitting GaN-based LEDs by Nakamura in 1991 and the development of high-power LEDs (HP-LEDs) in the same spectral region. [2] It is well known that the spectral properties of rare-earth ions with 5*d*–4*f* transitions (e.g., Eu^{2+}, Ce^{3+}) strongly depend on the surrounding environment (e.g., symmetry, covalence, coordination, bond length, site size, crystal-field strength, etc.), due to the fact that the 5*d* excited state is not shielded from the crystal field by the $5s^2$ and $5p^6$ electrons. [3-5]These phosphors can efficiently absorb in the near UV to blue spectral range and emit light in the visible range. And the small Stocks shift leads to high conversion efficiency. For a LED phosphor to be applied in commercial products, several criteria have to be met such as high efficiency in light conversion, high thermal quenching temperature, and the possibility to adjust the colour point by means of varying the chemical composition. Host lattices with a high degree of covalence and/or a large crystal field splitting at the site for which Eu^{2+} substitute can lead to efficient visible emission while absorbing light in the near UV to blue range of the electromagnetic spectrum. Presently $Y_3Al_5O_{12}:Ce^{3+}$ ($YAG:Ce^{3+}$) is applied in phosphor converted LEDs (pc-LEDs) as luminescent converter. [6,7] The most common commercial white LEDs (WLEDs) are combination of the blue-emitting InGaN chip and the yellow $YAG:Ce^{3+}$ phosphor . However, they have a low Colour Rendering Index（CRI） because of their lack of emission in the red region, and high color temperature due to the deficiency of emission in the visible spectrum. An alternative way to overcome this weakness is the incorporation with red phosphors. In this respect, a promising new class of LED phosphor materials is the nitridosilicates. The N^{3-} in this lattice is a soft Lewis base, which results in a high covalence. This shifts the energy of the 4*f*-5*d* absorption and emission for Eu^{2+} ions to sufficiently low energies.[8,9] In addition, nitridosilicates are known to be highly stable with oxidation and hydrolysis.[10] At present the commercial red nitrides phosphors are $CaAlSiN_3:Eu^{2+}$ [11.12] and $Sr_2Si_5N_8:Eu^{2+}$.[13-15] However, the sintering process of $CaAlSiN_3:Eu^{2+}$ phosphor needs critical preparation conditions (higher temperature, higher N_2 pressure, and air sensitive starting powders). For the latter**,** Piao *et al* [16] reported on the carbothermal reduction and nitridation method to synthesize $Sr_2Si_5N_8:Eu^{2+}$ phosphor. In this method, residual carbon is inevitably incorporated into the phosphor, which reduces its intensities of absorption and emission. Thus these nitrides phosphors cannot meet the requirements of orange-red phosphors at present. So there is a still need to discover novel orange-red phosphors. Currently, there is increasing interest in nitridosilicates $Ca_2Si_5N_8:Eu^{2+}$ due to its potential application in warm white LEDs. [17.18] And the preparation conditions were easier than the other commercial nitrides phosphors, such as the lower sintering temperature and pressure as well as the cheaper raw materials. Recently the researches on $Ca_2Si_5N_8:Eu^{2+}$ mainly concentrate on the different doping concentrations of Eu^{2+} to tune the emission color and increase the emission intensity. But there is no report on the cations substitution in $Ca_2Si_5N_8$ host to adjust the luminescence property. BaF_2 is a potential flux[19.20]. So we focus on the $Ca_2Si_5N_8:Eu^{2+}$ by using a BaF_2 as flux and cations substitution.

In this paper we report the possibility to tune the emission color of $Ca_2Si_5N_8:Eu^{2+}$ by incorporating BaF_2, to determine the

RSC Advances Accepted Manuscript

most promising way to design new compositions that can serve as efficient phosphors in pc-LEDs with a warmer color. The luminescence and thermal quenching properties have been estimated. And the mechanism for the emission increasing and wavelength shift after BaF_2 doping is discussed.

2. Experimental Section

2.1 Materials and Synthesis.

A series of nitridosilicate phosphors, $Ca_2Si_5N_8$:Eu^{2+} with different concentration of BaF_2 were prepared by Gas-Pressed Sintering. Stoichiometric amounts of powder BaF_2 (AR), Ca_3N_2 (Aldrich, >95.0%), Si_3N_4 (Aldrich, 99.5%), and Eu_2O_3 (Aldrich, 99.99%) were ground in an agate mortar for 30 min in a glove box to form a homogeneous mixture. The concentrations of both moisture and oxygen in the glovebox were <1 ppm. Thereafter, the powder mixture was transferred into a BN crucible and heated at 1500℃ for 4 h under high-purity nitrogen（99.9995%）atmosphere at a pressure of 0.2 MPa. The sintered products were ground again, yielding crystalline powder.

2.2 Characterization.

All measurements were made on finely ground powder. The phase purity of samples were analyzed by X-ray diffraction (XRD) using a Rigaku D/Max-2400 X-ray diffractometer with Ni-filtered CuKα radiation. Photoluminescence (PL) and PL excitation (PLE) spectra were measured at room temperature using an FLS-920T fluorescence spectrophotometer equipped with a 450W Xe light source and double excitation monochromators. High temperature luminescence intensity measurements were carried out by using an aluminum plaque with cartridge heaters; the temperature was measured by thermocouples inside the plaque and controlled by a standard TAP-02 high temperature fluorescence controller. X-ray photoelectron spectroscopy (XPS) measurements were performed on an ESCALAB250xi high-performance electron spectrometer using a monochromatized Al K*α* excitation source (hv = 1486.6 eV).

3. Results and Discussion

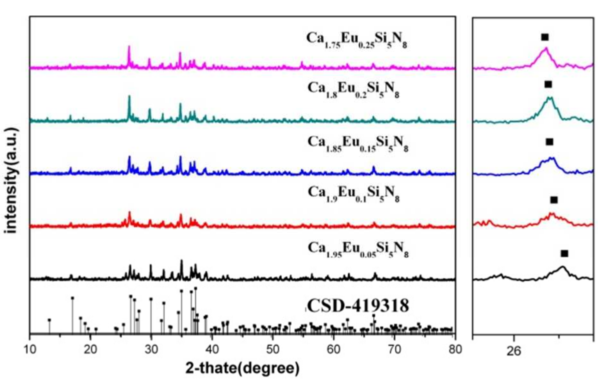

Fig. 1.XRD patterns of the $Ca_2Si_5N_8$:Eu^{2+} phosphors as a function of Eu^{2+} concentration.

Fig. 1 shows the XRD patterns of the $Ca_2Si_5N_8$:Eu^{2+} phosphors as a function of Eu^{2+} concentration. The detailed analysis of the XRD patterns of samples $(Ca_{1-x}Eu_x)_2Si_5N_8$ (x = 0.05, 0.1, 0.15, 0.2 and 0.25) shows that their phase compositions depend on the concentration of Eu^{2+}. When 0≤x≤0.15, the samples are almost the single phase of $(Ca_{1-x}Eu_x)_2Si_5N_8$ with a very small amount of α-Si_3N_4 as impurity. A further increase of Eu^{2+} concentration leads to the formation of α-Si_3N_4 and $EuSiO_3$, both as impurities. These observations indicate that the solubility of Eu^{2+} in $Ca_2Si_5N_8$ is very limited, probably, to a range of 0-0.15, i.e. 0≤x≤0.15, which is in consistent well with the result reported by Li *et al* [21] Such a limitation may be due to two reasons. One is the difference in the crystal structure that $Ca_2Si_5N_8$ is monoclinic while $Eu_2Si_5N_8$ is orthorhombic. The other is the difference between the ionic radii: the radius of Eu^{2+} (1.17 Å) (1 Å =0.1 nm) is obviously larger than that of Ca^{2+} (1.00 Å). [22]

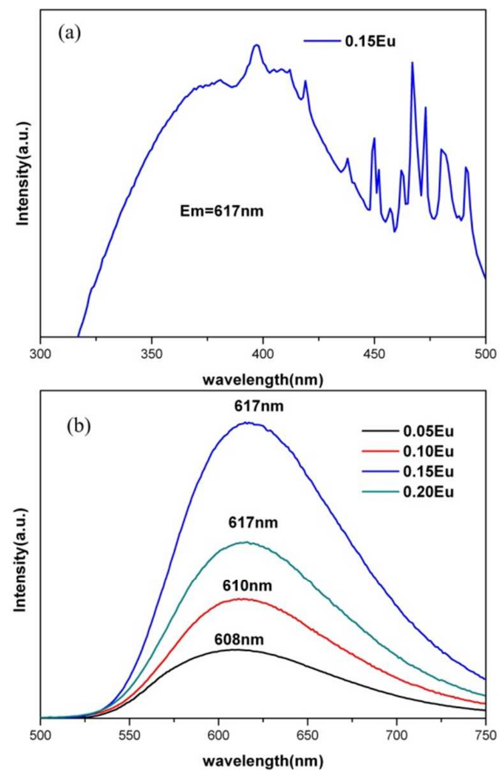

Fig.2. PLE spectrum (a) (monitored at 617 nm) and PL spectra (b) (excited at 460 nm) of the $Ca_2Si_5N_8$:Eu^{2+} phosphor with different Eu^{2+} contents.

Fig.2 (a) shows the excitation spectrum (λ_{em} = 617 nm) of $Ca_{1.85}Eu_{0.15}Si_5N_8$. The $Ca_{1.85}Eu_{0.15}Si_5N_8$ phosphor exhibited a typical broad excitation band resulting from the crystal field splitting of the 5*d* orbital due to the $4f^7$-ground state to the $4f^65d$-excited state of the Eu^{2+} ion electronic transitions.[23] Fig.2 (b) shows the emission spectra of the $Ca_{2-x}Eu_xSi_5N_8$ phosphors synthesized at 1500 °C for 4 h excited at 460 nm. The relative emission peak originated from the transitions of the 5*d* to the 4*f* states. As the Eu^{2+} doping concentration increases, the relative

This journal is © The Royal Society of Chemistry [year]
RSC Advances Accepted Manuscript

emission intensity increases continuously. The highest emission intensity is observed for the 0.15 mol of Eu^{2+} sample. However, when the Eu^{2+} concentration exceeds 0.15mol, there was a sudden decrease in the emission intensity due to concentration quenching.[24] As the Eu^{2+} contents increase, the distance between the Eu^{2+} ions becomes smaller, which leads to the probability of energy transfer among Eu^{2+} ions.[25] When the Eu^{2+} concentration increases, the emission band shifts to the red side. This may be ascribed to the lattice distortion caused by Eu^{2+} ions introducing the mismatch between the small Ca^{2+} and large Eu^{2+} ionic radius in the lattice.[26]

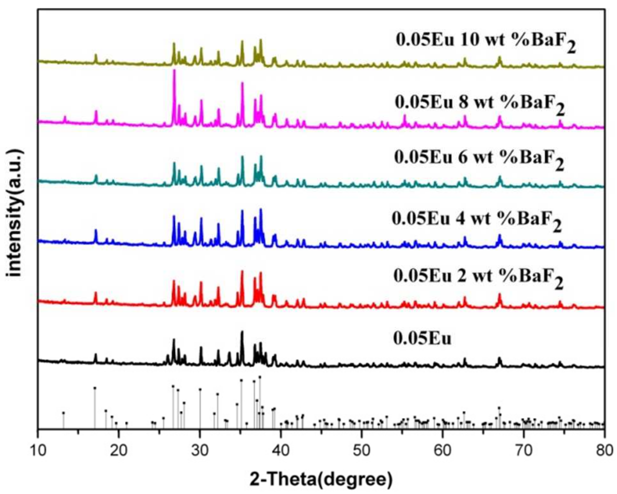

Fig. 3. XRD patterns of the $Ca_2Si_5N_8$:Eu^{2+} phosphors with different concentrations of BaF_2.

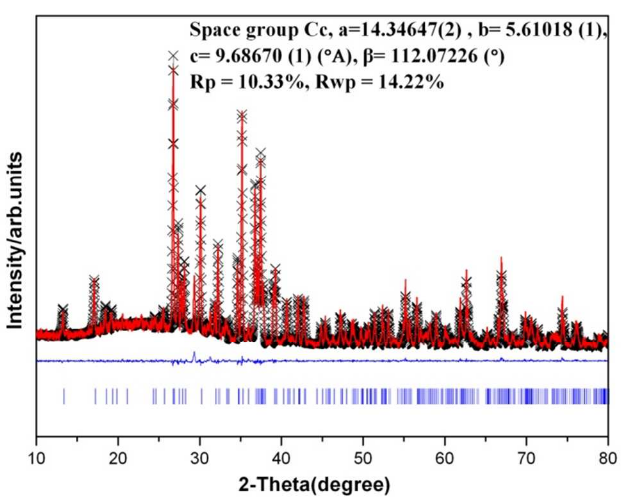

Fig. 4.Rietveld refinement results of the XRD patterns of the $Ca_2Si_5N_8$:Eu^{2+} with 8 wt % BaF_2, including the experimental and calculated intensities as well as differences in intensity between experimental and calculated data.

Table 1 The refined structure parameters of BaF_2 doped $Ca_2Si_5N_8$:Eu^{2+}.

Atom	Site	x/a	y/b	z/c
Ca1	0.95	-0.00658	0.75426	0.05207
Ba	0.05	-0.00658	0.75426	0.05207
Ca2	1	0.61050	0.73056	0.26069
Si1	1	0.05412	0.79009	0.41769
Si2	1	0.75221	0.19935	0.34537
Si3	1	0.76388	0.51462	0.11491
Si4	1	0.35762	0.21081	0.42527
Si5	1	0.85405	0.02307	0.17204
N1	1	0.94559	0.55880	0.44382
N2	1	0.12258	0.12972	1.08940
N3	1	0.81030	0.25662	0.23980
N4	1	0.79107	0.85548	0.15102
N5	1	0.98494	0.98304	0.27838
N6	1	0.86102	0.17452	1.06034
N7	1	0.62438	0.04133	0.36236
N8	1	0.79600	0.49423	0.41610

Fig. 3 shows the XRD patterns of $Ca_{1.95}Eu_{0.05}Si_5N_8$ with different weight of BaF_2. When BaF_2 is doped, the sample is the single phase of $(Ca_{1-x}Eu_x)_2Si_5N_8$. The positions of the peaks move to lower angles and the volumes of lattice parameters show smooth evolution as the BaF_2 content increases, which means that the higher the Ba^{2+} content is, the larger the lattice parameters are(sees in supporting information Fig. S1 (ESI†)) and the Ba^{2+} should occupy the Ca^{2+} position. The crystallinity has been improved with the addition of BaF_2. When adding 8 wt % BaF_2 is added, the crystallinity of the sample reaches the highest. And the crystallinity begins to decline when the content of BaF_2 exceeds 8 wt %.

Fig. 4 shows the experimental, calculated, and difference results of Rietveld refinement XRD patterns of $Ca_{1.95}Eu_{0.05}Si_5N_8$ with 8 wt % BaF_2 at room temperature. The crystal structure of $Ca_{1.95}Eu_{0.05}Si_5N_8$ with 8 wt % BaF_2 was analyzed by the Materials Studio program on the basis of the XRD data. The pattern factor R_p, and the weighted pattern factor R_{wp}, are 10.33% and 14.22%, respectively. The XRD patterns of $Ca_{1.95}Eu_{0.05}Si_5N_8$ with 8 wt % BaF_2 obtained herein indicate that single phases are formed. The $Ca_{1.95}Eu_{0.05}Si_5N_8$ with 8 wt % BaF_2 synthesized crystallized as a monoclinic structure with the space group of Cc. The refined structure parameters of BaF_2 doped $Ca_2Si_5N_8$:Eu^{2+} is given in Table 1.

RSC Advances Accepted Manuscript

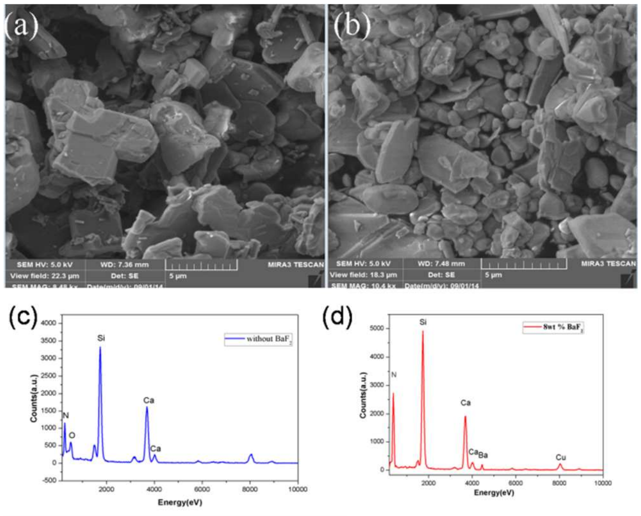

Fig. 5. SEM and EDX spectra of the (a, c) $Ca_{1.95}Eu_{0.05}Si_5N_8$ and (b, d) $Ca_{1.95}Eu_{0.05}Si_5N_8$ with 8 wt% BaF_2.

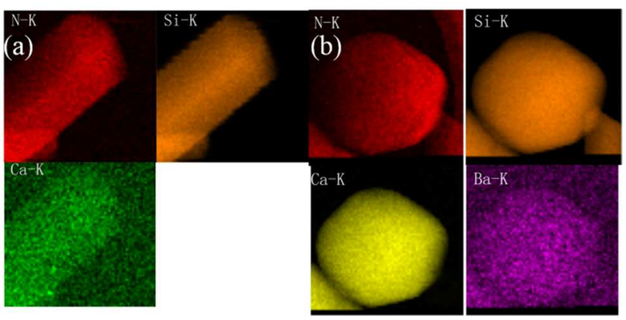

Fig. 6 Elemental mappings of $Ca_{1.95}Eu_{0.05}Si_5N_8$ and $Ca_{1.95}Eu_{0.05}Si_5N_8$ with 8 wt% BaF_2 .

When compared the two images of (a) $Ca_{1.95}Eu_{0.05}Si_5N_8$ and (b) $Ca_{1.95}Eu_{0.05}Si_5N_8$ with 8 wt% BaF_2 in Fig. 5, we can find that the addition of the BaF_2 in the host is helpful for enhancing the crystallization degree and decreasing surface defects. This indicates that the $Ca_{1.95}Eu_{0.05}Si_5N_8$ phosphor has a good dispersion, a regular shape, and the particle size of the synthesized powder was about 6–12μm. The corresponding EDX spectra analysis (Fig. 5(c, d)) and Elemental mappings (Fig. 6(a, b)) indicates that the products have a chemical composition of Ca, Si, O and N and Ca, Ba, Si, O and N. And the Ba^{2+} is incorporated into the $Ca_{1.95}Eu_{0.05}Si_5N_8$.

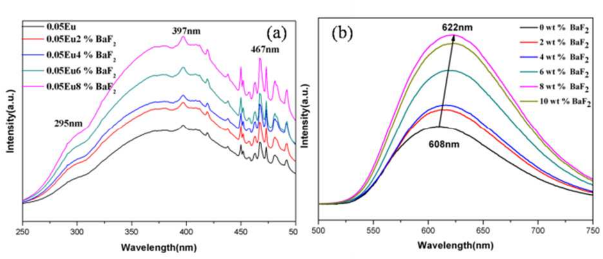

Fig.7. PL/PLE spectra of $Ca_{1.95}Eu_{0.05}Si_5N_8$ with different weight of BaF_2.

Table 2 Excitation, emission, centre of gravity and Stokes shift crystal filed splitting of $Ca_{1.95}Eu_{0.05}Si_5N_8$ with different weight of BaF_2

Samples	λex(nm)	λem(nm)	Center of gravity(cm^{-1})	Stocks shift(cm^{-1})
Without BaF_2	295,397,467	608	26830	4966
2% BaF_2	295,397,467	613	26830	5100
4% BaF_2	295,397,467	615	26830	5153
6% BaF_2	295,397,467	618	26830	5232
8% BaF_2	295,397,467	622	26830	5336

Fig.7 shows the excitation and emission spectra of $Ca_{1.95}Eu_{0.05}Si_5N_8$. It is obvious that all the spectral features of the as-synthesized samples are similar. The excitation spectra consist of three broad bands peaking at about 295, 397 and 467 nm, which mainly arise from the $4f^65d^1$multiplets of Eu^{2+} excitation states. And the remarkable enhancement of the emission intensity is observed with increasing the content of BaF_2. After incorporating 8 wt % BaF_2, the emission intensity reaches twice than that of the sample without BaF_2. In addition, it is noticeable that the emission peak of the Eu^{2+} shifts to longer wavelength (608nm to 622nm) with increasing the concentration of BaF_2. This would be beneficial to the color point tuning. The excitation, emission, centre of gravity and Stokes shift crystal filed splitting of $Ca_{1.95}Eu_{0.05}Si_5N_8$ with different weight of BaF_2 are listed in Table 2 . The enhancement can be explained by the fluxing agent (BaF_2). The redshift could be explained by the fact that the $Ca_2Si_5N_8:Eu^{2+}$ structure is preserved while a part of the Ca^{2+} ions are replaced by the larger Ba^{2+} ions. To accommodate these larger cations, the distance between Ca^{2+} (or Eu^{2+}) and the anions could not increase or even become slightly smaller, thus leading to the increase of the crystal field splitting, and then causing a red shift of the emission. [27]

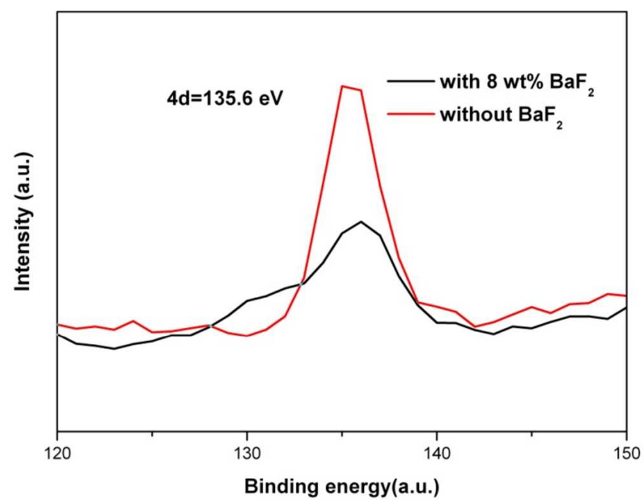

Fig.8. XPS survey spectrum of $Ca_{1.95}Eu_{0.05}Si_5N_8$ with and without BaF_2.

Table 2 XPS quantitative results of $Ca_{1.95}Eu_{0.05}Si_5N_8$ with and without BaF_2

Peak	Position BE （eV）	Atomic Conc%	Mass Conc%

RSC Advances Accepted Manuscript

This journal is © The Royal Society of Chemistry [year]

N	402	15.44	10.23
O	536	21.34	16.16

Peak	Position BE （eV）	Atomic Conc%	Mass Conc%
N	402	18.81	12.68
O	536	20.56	15.84

Fig.8 shows the XPS of $Ca_{1.95}Eu_{0.05}Si_5N_8$ with 8 wt % BaF_2 and without BaF_2. The lattice parameters are greatly affected by the occupation of Eu^{2+} and Ba^{2+} ions in the critical structure, which depends on the difference in electronegativity and ionic radii compared with the replaced ions. The two ions have a similar possibility to replace Ca^{2+} ions and be incorporated into the structure. However, it is well known that the vacancy formation caused by charge imbalance and lattice strain can self-limit the inclusion of guest ions into a host lattice. [28] Thus there is a propensity for the ions to migrate to less strained surface sites, rather than incorporate in the crystal lattice,which can be confirmed by XPS data. In Fig. 6, the peak at about 135.6 eV attributed to Eu_{4d} is assigned to Eu_2O_3 which was formed on the surface of the sample. That means more Eu^{2+} ions are incorporated into the lattice, lead to emission intensity increasing and red shift of the emission. Another reason is that the N/O ratio is higher in the $Ca_{1.95}Eu_{0.05}Si_5N_8$ with 8 wt % BaF_2 sample. The nitrogen ion (N^{3-}) has a higher effective charge compared with the oxygen ion (O^{2-}), and the electronegativity of nitrogen (3.04) is smaller than that of oxygen (3.50). Therefore, coordinating with nitrogen would cause a stronger nephelauxetic effect (covalence), the centre of gravity of the 5d states of the activator ions shift to longer wavelength, and the crystal-field splitting larger than that in a similar oxygen environment, [29.30] which leads to the red shift of the emission.

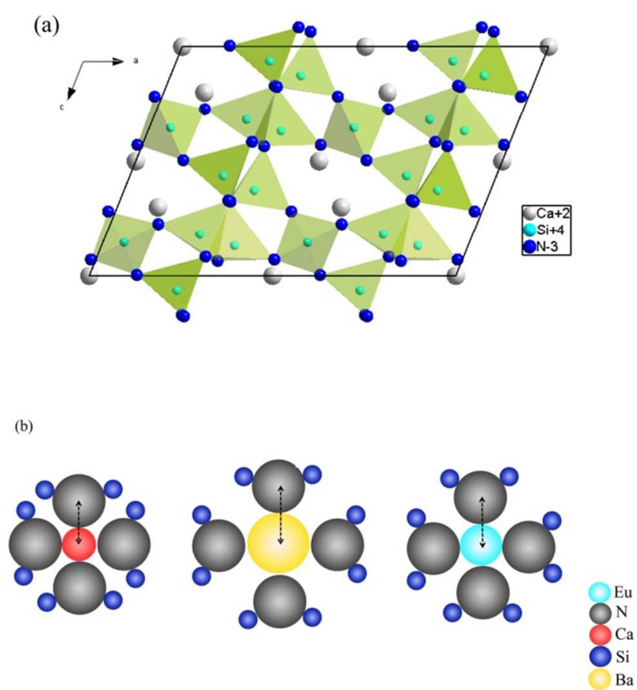

Fig.9. (a) Crystal structure of $Ca_2Si_5N_8$ viewed along [010]. (b) The proposed model of substitution of Eu^{2+} and Ba^{2+} for Ca^{2+}.

Fig 9(a) shows the crystal structure of $Ca_2Si_5N_8$ viewed along [010] and Fig 9 (b) depicts the proposed model of substitution of Eu^{2+} and Ba^{2+} for Ca^{2+}. Furthermore, a random ion displacement model can be used to clarify the modification of the lattice. This allows the use of an analysis similar to Vegard's law, which is an empirical law that relates the statistical substitution of a guest ion into the host lattice with the experimentally observed degree of lattice change with increasing defect ion concentration. Statistical substitution into a lattice site is predicted to lead to a lattice contraction for smaller ions and a lattice expansion for larger ions. When there are only Eu^{2+} ions doped in the structure, the cell lattice will be expanded, since the radius of Eu^{2+} ions is larger than that of Ca^{2+} ions. A strain may arise in the lattice around the Eu^{2+} ions, and may limit the stability of the Eu^{2+} ions that had been incorporated into the lattice. Then, when Ba^{2+} was doped into the structure, the Ba^{2+} ions with larger radius than that of Eu^{2+} could make the lattice expand. So more Eu^{2+} would incorporate into the lattice because of the larger lattice expended by Ba^{2+}.This means that the structure doped with Ba^{2+} ions can make more Eu^{2+} ions incorporate into the lattice.

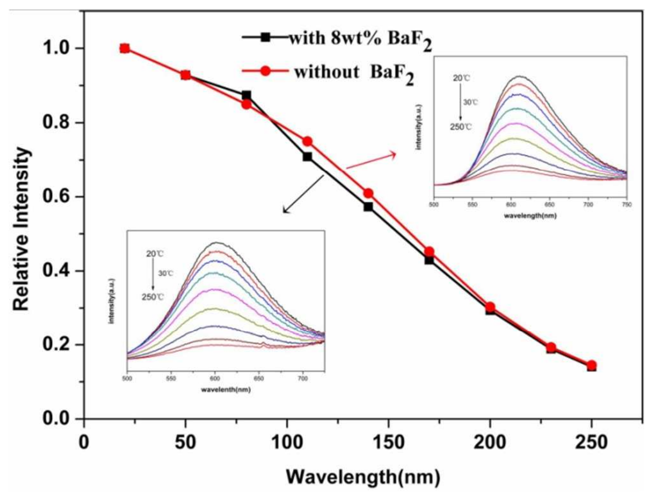

Fig.10. Temperature dependent integrated emission intensities of $Ca_{1.95}Eu_{0.05}Si_5N_8$ with and without 8 wt % BaF_2.（The inset show the emission spectra with increasing temperature）

Fig 10 shows the temperature dependence of the integrated emission intensity for $Ca_{1.95}Eu_{0.05}Si_5N_8$ with and without 8 wt % BaF_2, which shows an identical thermal stability. It is believed that thermal ionization is responsible for quenching of the luminescence of Eu^{2+} at high temperatures in $Ca_2Si_5N_8$ host, [17] because the excited 5*d* electrons are easily ionized by the absorption of thermal energy and entrance into the bottom of the conduction band of the host through the top of the Eu^{2+} excitation levels. At 200 °C, the integral emission intensity of the both phosphors is about 30 % of that measured at room temperature.

RSC Advances Accepted Manuscript

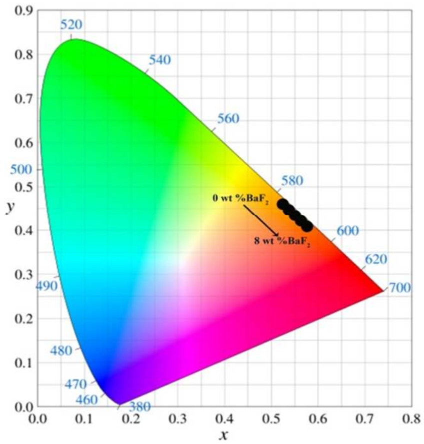

Fig.11 CIE chromaticity coordinates of $Ca_{1.95}Eu_{0.05}Si_5N_8$ with different BaF_2（0 wt%-8 wt%）

Fig 11 represents the Commission International de I'Eclairage (CIE) chromaticity coordinates for $Ca_{1.95}Eu_{0.05}Si_5N_8$ with different amounts of BaF_2 (0 wt %-8 wt %). With increasing the content of Ba^{2+}, the chromaticity coordinates (x, y) vary systematically from (0.556, 0.437) to (0.591, 0.407), corresponding to color points of the samples change gradually from orange-yellow to orange-red. Therefore, it is expected that the white light with good rendering could be obtained when the tunable emission phosphors $Ca_{1.95}Eu_{0.05}Si_5N_8$ with different amounts of BaF_2（0 wt %-8 wt %）for white LEDs.

4. Conclusions

A remarkable orange-red nitridosilicate phosphor $Ca_{1.95}Eu_{0.05}Si_5N_8$ with 8 wt % BaF_2 was synthesized by Gas-Pressed Sintering at 1500℃ using the raw materials BaF_2, Ca_3N_2, Si_3N_4, and Eu_2O_3. This method promises the use of inexpensive, commercially available and powder handling at ambient pressure, thus offering a simple, efficient, and high-yield way to obtain orange-red emitting phosphors. The color of the emission can be tuned with adding BaF_2 into the $Ca_2Si_5N_8:Eu^{2+}$ host lattice. We have demonstrated that adding BaF_2 can make better single phase, emission peak shift to longer wavelength (608 nm to 622 nm) and significantly enhance the emission of $Ca_2Si_5N_8:Eu^{2+}$ phosphors. This is mainly due to the fact that the lattice structure of $Ca_2Si_5N_8:Eu^{2+}$ phosphors can be modified and the solubility of the Eu^{2+} ions can be increased by adding BaF_2. More Eu^{2+} ions would incorporate the lattice because of the larger lattice expended by Ba^{2+}. This novel $Ca_2Si_5N_8:Eu^{2+}$ with 8 wt % BaF_2 phosphor is expected to be useful for phosphor converted white LEDs.

5. Acknowledgment

This work is supported by Specialized Research Fund for the Doctoral Program of Higher Education (no. 20120211130003) and the National Natural Science Funds of China (Grant No. 51372105).

6. Notes and references

[1]E. F. Schubert and J. K. Kim, *Science.*, 2005, **308**, 1274–1278.
[2]Nakamura, S. Jpn. *J. Appl. Phys* 1991, **30 (10A)**, L1705.
[3] G. Blasse and B. C. Grabmaier, Luminescent Materials, Springer, 1994. vol. 44.
[4]J. W. H. van Krevel, H. T. Hintzen, R. Metselaar and A. Meijerink, *J. Alloys Compd*., 1998, **268**, 272-277.
[5]R. J. Xie, N. Hirosaki and M. Mitomo, *J. Electroceram*., 2008, **21**, 370-373.
[6]P. Schlotter, J. Baur, C. Hielscher, M. Kunzer, H. Obloh, R. Schmidt and J. Schneider,*J. Mater. Sci. Eng. B.*, 1999, **59**,390－396
[7]Hu, Y. Zhuang, W.Ye, H. Zhang, S. Fang, Yand Huang X, *J. Lumin*. ,2005, **111**, 139-145.
[8]J. Ballato, J. S. Lewis, III and P. Holloway, *Mater. Res. Bull*.,1999, **24(9)**, 51.
[9]Z. J. Zhang, Otmar M. ten Kate, A. Delsing, Erik van der Kolk, Peter. H. L. Notten and Hubertus T. Hintzen, *J. Mater. Chem*.,2012,**22**,9813-9820
[10]Cora Hecht and Schnick, W. Int. *Chem. Mater.*, 2009, **21 (8)**, 1595–1601
[11]X. Piao, K. Machida, T. Horikawa, H. Hanzawa, Y. Shimomura and N. Kijima, *Chem. Mater.*, 2007, **19**, 4592–4599.
[12]Y. Li, N. Hirosaki, R. Xie, T. Takeda and M. Mitomo, Chem. Mater. 2008, 20, 6704–6714.
[13]Xianqing Piao and Ken-ichi Machida. *J. Lumin*. , 2010,**13**,08-12.
[14]Hayk Nersisyan, Hyung Il Won and Chang Whan Won. *Chem. Commun*., 2011,**47**,11897-11899.
[15]Y.Q. Li and H.T.Hintzen, *J. Solid State Chem.*, 2008,**181**,515-524.
[16] Xianqing Piao, Ken-ichi Machida, Takashi Horikawa and Hiromasa Hanzawa. *J. Electrochem. Soc.* 2008, **155**, 1,17-22.
[17]Xiao-Dan Wei and Quan-Lin Liu, *Chin. Phys. Soc.*,2009,**18**,3555-3563
[18]BingfuLei,Yasuo Shimomura and Hajime Yamamoto**,** *J. Electrochem. Soc*., 2010, **157**, J196-J201.
[19] Sang Ho Lee, Hye Young Koo, Dae Soo Jung, Jin Man Han, Yun Chan Kang.*Optical Materials*.**,** 2009, **31**, 870–875
[20] Sang Ho Lee, Dae Soo Jung, Jin Man Han, Hye Young Koo, Yun Chan Kang. *J. Alloys Compd*., 2009, 477, 776–779
[21] Y Q Li, de With G and H T Hintzen, *J Alloys Compd*., 2006,**417**,273
[22] R. D. Shannon, *Acta Cryst*., 1976, **A32**, 751-767
[23] Y Gu, Q Zhang, Y Li, H Wang, RJ Xie, *Mater Lett.,* 2009,**63**,1448–50.
[24] D. L. Dexter and James H. Schulman *J. Chem. Phys.*, 1954, **22**, 1063
[25] Van Uitert LG, *J. Electrochem Soc* 1967, **114**, 1048－1053.
[26]H. Zhang, T. Horikawa, H. Hanzawa, A. Hamaguchi and K.-I. Machida,*J. Electrochem. Soc*., 2007, **154(2)**, J59–J61.
[27]Volker Bachmann and Andries Meijerink, *Chem. Mater.*, 2009, **21**, 316–325
[28]Yunxin Gu, Qinghong Zhang, Yaogang Li, Hongzhi Wang, R.J. Xie , *Mater.Lett.*, 2009, **63**, 1448－1450
[29]Z. Y. Zhao, Z. G. Yang, Y. R. Shi, C. Wang, B. Liu, G. Zhu and Y. H. Wang, *J. Mater. Chem.C.*, 2013, **1**, 1407-1412
[30]C. W. Yeh, W. T. Chen, R. S. Liu, S. F. Hu, H. S. Sheu, J. M. Chen, and H. T. Hintzen, *J. Am. Chem. Soc.*, 2012, **134**, 14108−14117.

RSC Advances Accepted Manuscript

 This journal is © The Royal Society of Chemistry [year]